

LNF-96/003

The KLOE drift chamber

A. Calcaterra

Nuclear Instruments & Methods A 367, 104-107, (1995)



ELSEVIER

The KLOE drift chamber

A. Calcaterra

*Laboratori Nazionali di Frascati dell'INFN, Frascati, Italy*For the KLOE Collaboration¹

Abstract

The KLOE drift chamber is a cylinder of ~ 2 m radius and ~ 3.3 m long, providing an adequate path for K_L decays. The tracking volume is surrounded by a $15 X_0$ em calorimeter and a superconducting coil providing a 0.6 T field. Spherical end walls hold the tension of $\sim 50\,000$ wires, with good transparency, $\leq 0.1 X_0$, to photons from π^0 decays. Alternating stereo wires only, with constant radial displacement at the center, provide a uniform filling with approximately square cells. A He- iC_4H_{10} gas mixture and Al field wires are used to minimize multiple scattering. The chamber point resolution in r, ϕ is significantly better than $200\ \mu\text{m}$ resulting in a $K_L \rightarrow \pi^+ \pi^-$ vertex accuracy of $\sigma_{x,y(z)} \leq 0.5(1-2)$ mm. The K^0 mass resolution is $\sigma_M \sim 1\ \text{MeV}/c^2$.

1. Introduction

The major aim of the KLOE experiment at DAΦNE, the Frascati ϕ -factory, is the study of CP violation at sensitivities of $O(10^{-4})$ [1,2]. To this end systematic effects must be controlled to unprecedented accuracy. As described in Refs. [1,2] $K^0 \rightarrow \pi^0 \pi^0$ decays are detected by a hermetic electromagnetic calorimeter, EmC (Fig. 1), surrounding the tracking volume. Detection and reconstruction of $K_L \rightarrow \pi^+ \pi^-$ decays is the most demanding task for the chamber. Errors in vertex reconstruction affect counting of decays in any given fiducial volume. The required resolution is ~ 1 mm. Background decays, e.g. $K_{\mu 3}$, must be very efficiently rejected. To achieve the above at a ϕ -factory is strongly influenced by the following points. The mean decay path of K_L 's from ϕ decays at rest is ~ 3.5 m, therefore the K_L decay vertices populate a large volume, as shown in Fig. 2. The spectrum of pions from $K_L \rightarrow \pi^+ \pi^-$ is essentially flat between 150 and 270 MeV/ c and for $K_L \rightarrow \pi^+ \pi^- \pi^0$ the average momentum is only ~ 100 MeV/ c . The large opening angle between pions in $K_L \rightarrow \pi^+ \pi^-$, 160° , makes vertex reconstruction hard. All the above points are reflected in the choice of chamber dimension, its mechanical structure, the cell shape, the gas and the magnetic field value. The need for a large fiducial volume, yet smaller than the radius R of the drift chamber, leads to the choice of $R \sim 2$ m. Low Z materials must be used for the chamber structure and control of multiple

scattering requires the use of helium. A summary of the performance required of the KLOE tracking device is given in Table 1 [3].

2. Chamber design

The design of the large tracking chamber for the KLOE detector is driven for the most part by what follows from the above considerations:

- 1) Maximize the homogeneity and isotropy of the active tracking volume because of the long decay path of the K_L and the isotropic angular distribution of the charged decay products.
- 2) Achieve a high and well controlled efficiency for the reconstruction of $K_L \rightarrow \pi^+ \pi^-$ decays.
- 3) Optimize resolution at low momentum values.
- 4) Minimize the number of wires, both sense and field, in order to ease the difficulties of building a transparent chamber shell, minimize multiple scattering and maintain the electronics channels count within reasonable limits.

2.1. Mechanical structure

All walls of the KLOE chamber must be as thin as possible in order to minimize photon conversions before the EmC and multiple scattering and energy losses of charged particles entering the chamber. This is hardest to achieve for the end plates. Flat plates are unacceptably thick, while thin conical or spherical plates can carry the load of the wires, with deformations of $O(1\ \text{mm})$. By properly attaching the end plate's outer rim to a torsionally

¹ The members of the KLOE Collaboration are listed in the Appendix.

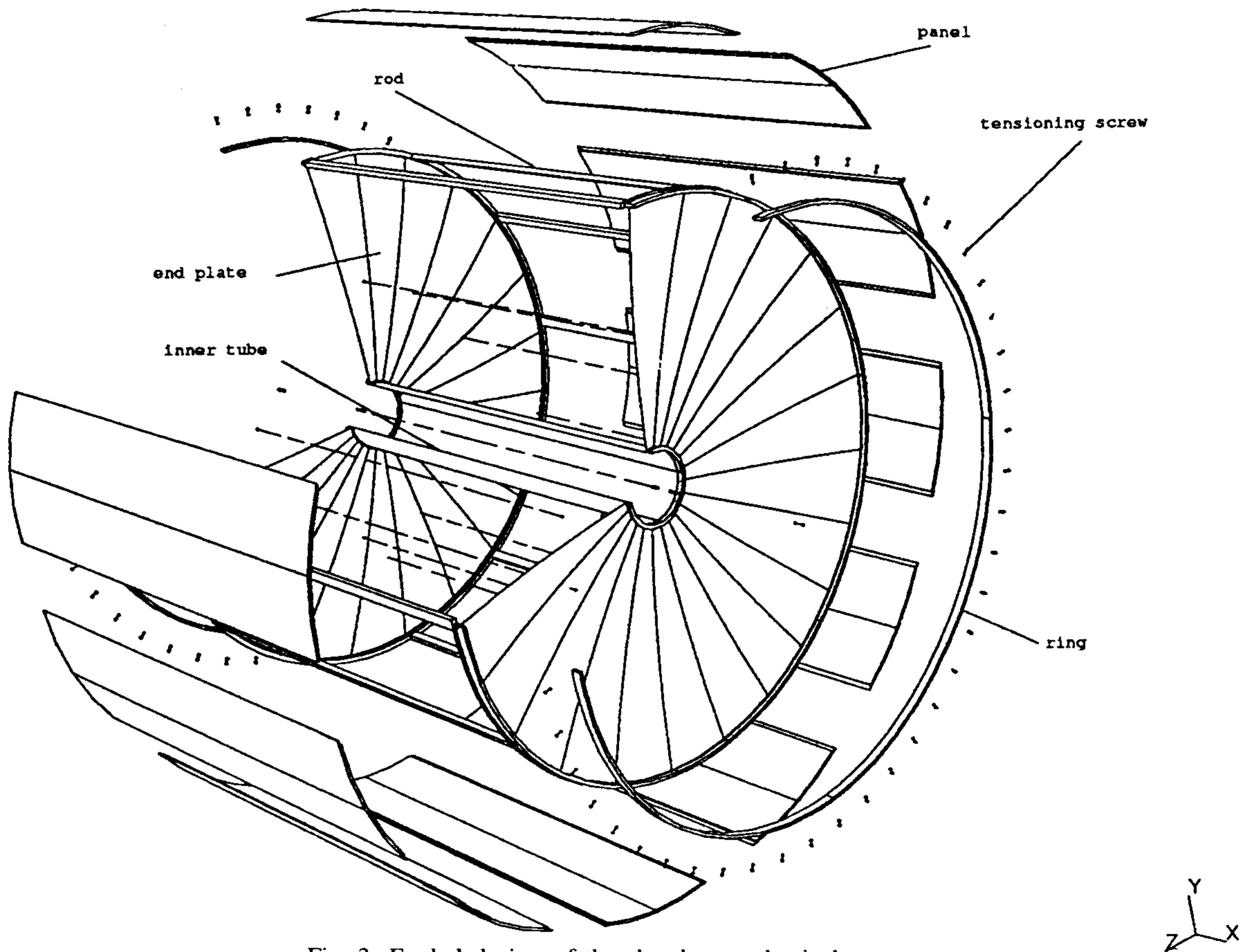


Fig. 3. Exploded view of the chamber mechanical structure.

prototypes in various beams [5]. In small prototypes we find (see Fig. 4) that a 90–10 mixture of He- iC_4H_{10} whose radiation length is $X_0 = 1300$ m performs quite satisfactorily giving the required resolution with efficiency $>99\%$. Addition of sense (W, diameter $25 \mu\text{m}$) and field wires (Al, diameter $80 \mu\text{m}$) to the above gas mixture results in a

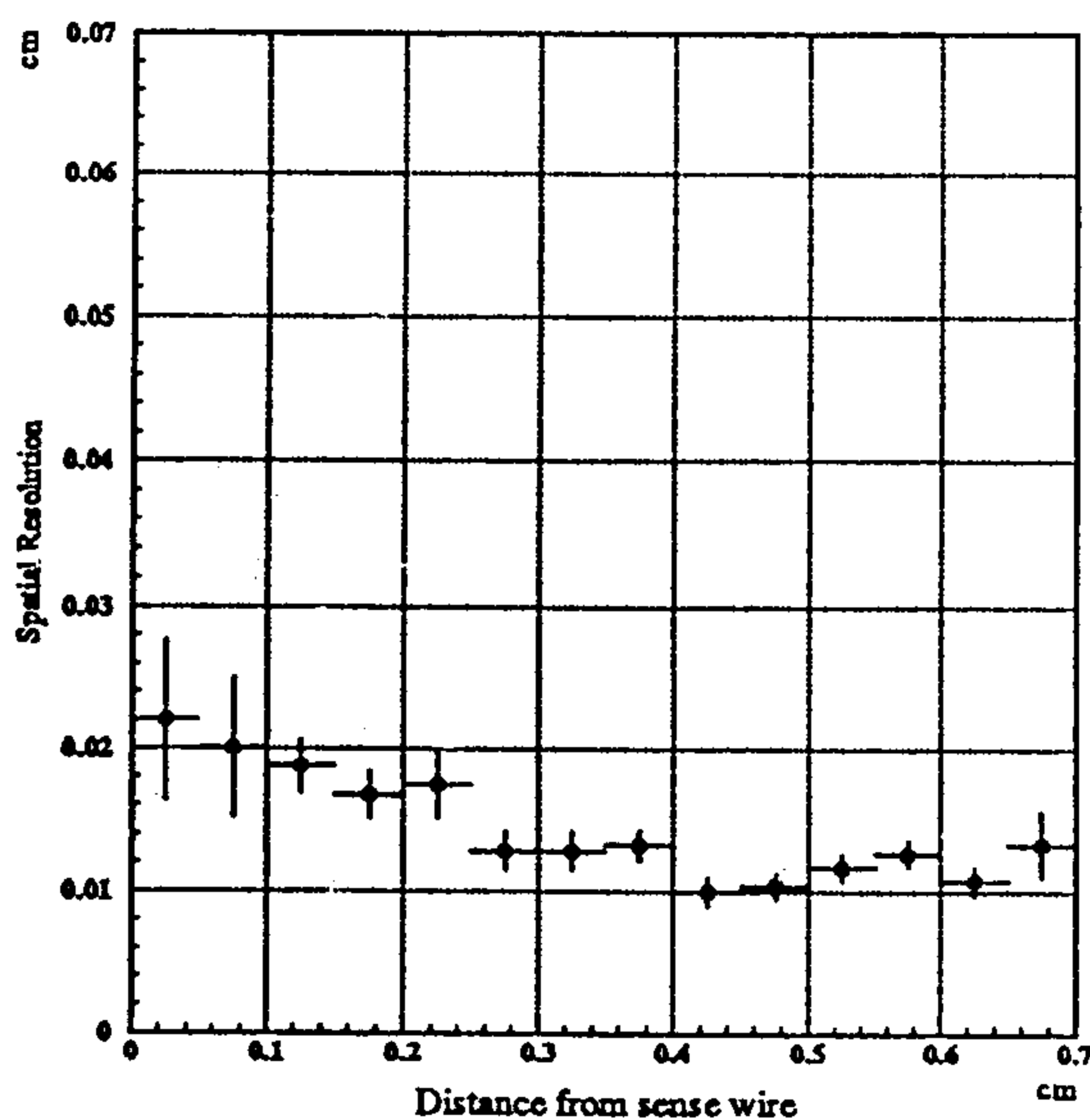


Fig. 4. Prototype spatial resolution.

value $\langle X_0 \rangle = 900$ m over the chamber volume. The drift velocity, at an operating voltage of 1.9 kV m , is not saturated over most of the cell, and corrections must be made iteratively in the track fit, according to drift distance and crossing angle. The low drift velocity in He gas mixtures [6], and the correspondingly small Lorentz angle, implies that the magnetic field will only change the time-space correlation without loss in either resolution or efficiency.

2.3. Cell design (see Fig. 5)

The uniform distribution of K_L decay vertices and secondary tracks in the chamber volume requires a constant size drift cell. This is achieved by using only alternating stereo layers, with constant inward radial displacement at the chamber center. This results in a stereo angle which increases with radius, $50 \text{ mrad} \leq \theta_{st} \leq 120 \text{ mrad}$, and an approximately constant, square cell shape along z , with constant wire gain. The choice of a relatively big drift cell of $3 \times 3 \text{ cm}^2$ helps in reducing the total amount of material in the chamber, while still maintaining a proper time-space correlation over most of the cell. Simulation studies show that the single track losses would be slightly smaller for a $2 \times 2 \text{ cm}^2$ cell, that the overall loss for full $K_L \rightarrow \pi^+ \pi^-$ reconstruction is

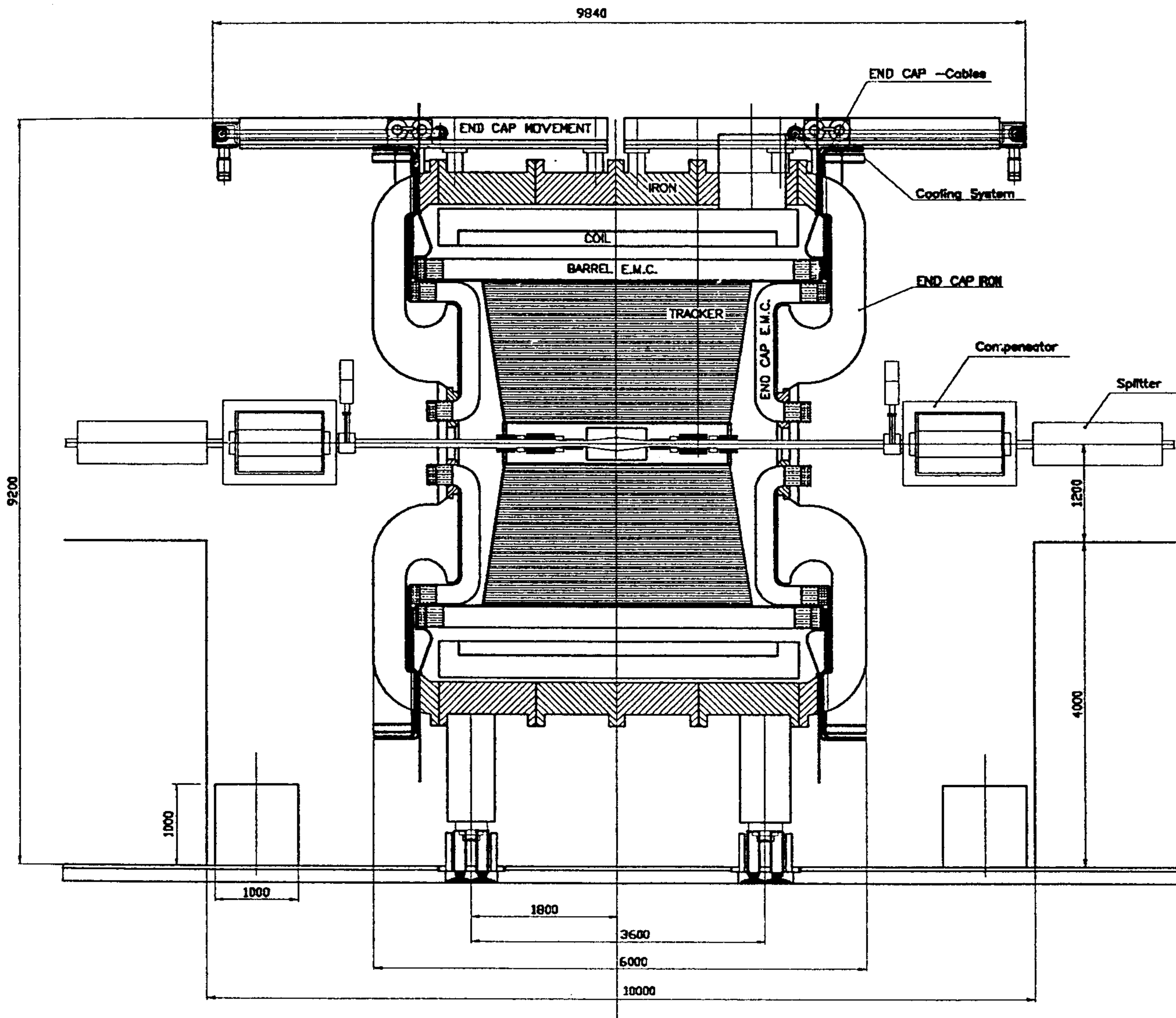
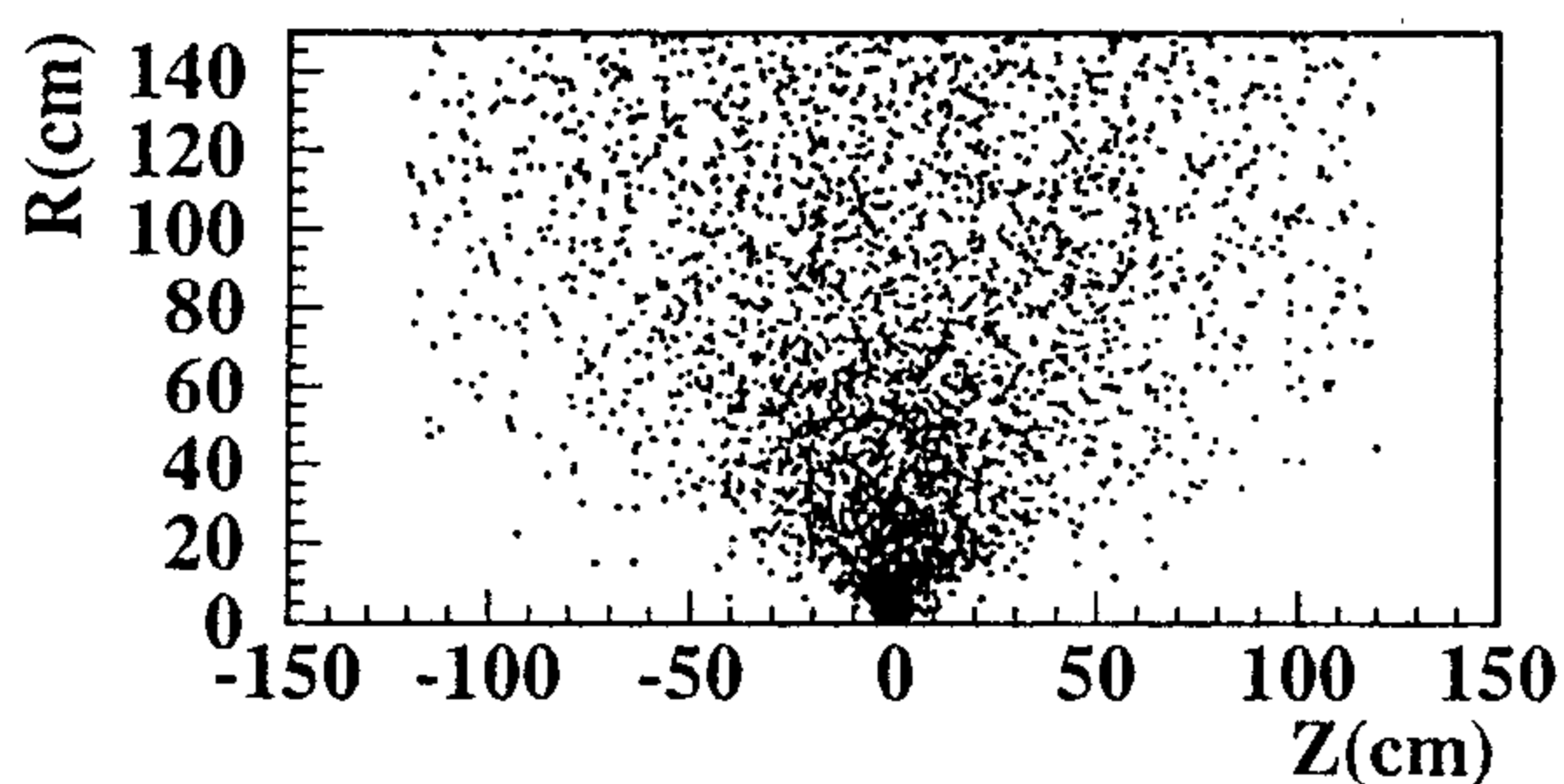


Fig. 1. Cross section of the KLOE detector.

Fig. 2. R - Z distribution of K_L decay vertices.Table 1
Drift chamber performance

Parameter	Value
$\delta_{x,y}$	200 μm
δ_z	2 mm
δP_i	$0.5\% \times P_i$
$\delta(\tan(\theta))$	$(3.5 \oplus 2.5) \times 10^{-4}$
$\delta(M_{\pi^+\pi^-})$	1 MeV/c^2

stiff ring, deformation under load is strongly reduced. Better yet is to apply at the plate rim a pull tangential to its surface, a solution adopted in the KLOE chamber design [4] (see Fig. 3).

The two end plates of the chamber are kept apart by twelve rods attached to an outer ring. Gas seal is completed by twelve panels which will be mounted after chamber stringing and an inner cylinder. This last is attached to the end plates via two rings at the center of the plates which also provide support for the low β insertion. Panels and inner cylinder carry no loads in our design. The chamber, with spherical end plates, built with either Al- or C-fibers, can withstand the tension of $\sim 50\,000$ wires, with good transparency ($\leq 0.1 X_0$) to photons from π^0 decays.

2.2. Gas choice

We have studied the performance of several helium gas mixtures, both with computer simulations [3] and with

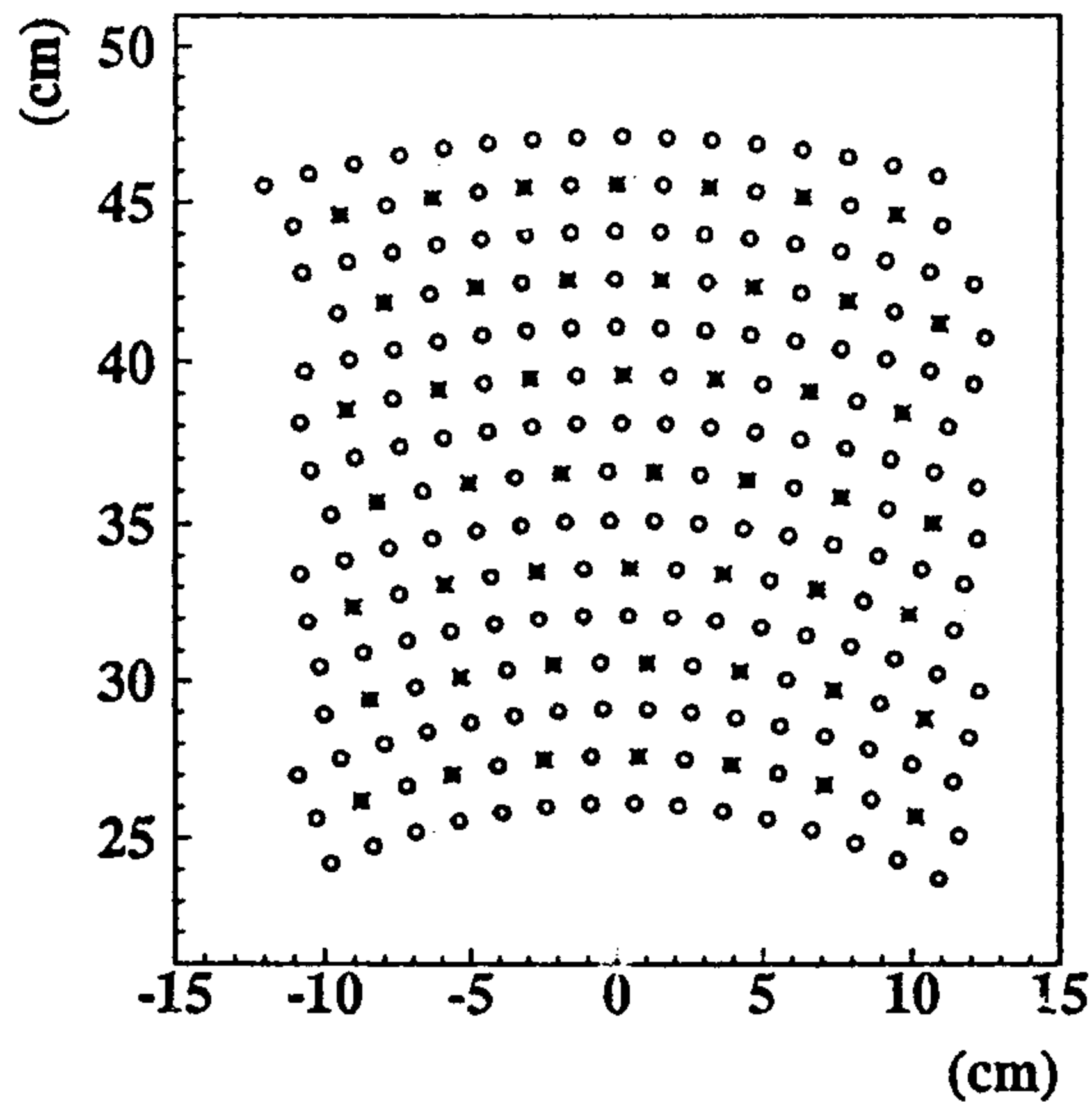


Fig. 5. Cell structure at $z = 0$.

larger by ~ 1.5 with a $3 \times 3 \text{ cm}^2$ cell. However, given the large difference in number of wires for the two cases, $(3/2)^2$, we feel that the larger cell is an acceptable compromise. Good tracking and vertexing for $K_S \rightarrow \pi^+ \pi^-$ is obtained using twelve layers of $1.5 \times 1.5 \text{ cm}^2$ cells in the inner part of the chamber, followed by layers of 3×3 cells. Realistic studies of $K_{\mu 3}$ contamination removal have shown that the rejection factor at a field value of 6 kG is approximately 4.5×10^{-4} with a $\pi^+ \pi^-$ signal efficiency of 98.8% [3].

Appendix: Members of the KLOE Collaboration

A. Aloisio^e, A. Andryakov^b, A. Antonelli^b, M. Antonelli^b, F. Anulli^b, C. Avanzini^h, D. Babusci^b, C. Bacci^j, R. Baldini-Ferrolì^b, G. Barbiellini^m, M. Barone^h, K. Barth^c, V. Baturin^e, H. Beker^h, G. Bellettini^g, G. Bencivenni^b, S. Bertolucci^b, C. Bini^h, C. Bloise^b, V. Bocciⁱ, V. Bolognesi^g, F. Bossi^b, P. Branchini^k, L. Bucci^h, A. Calcaterra^b, R. Caloi^h, P. Campana^b, G. Capon^b, M. Carboni^b, G. Cataldi^d, S. Cavaliere^c, F. Ceradini^j, L. Cerritoⁱ, M. Cerù^h, F. Cervelli^g, F. Cevenini^c, G. Chiefari^c, G. Ciapetti^h, M. Cordelli^b, P. Creti^d, A. Doria^c, F. Donno^b, R. De Sangro^b, P. De Simone^b, G. De Zorzi^h, D. Della Volpe^e, A. Denig^c, G. Di Cosimo^h, A. Di Domenico^h, E. Drago^c, V. Elia^d, O. Erriquez^a, A. Farilla^a, G. Felici^b, A. Ferrari^g, M.L. Ferrer^b, G. Finocchiaro^b, D. Fiore^c, P. Franzini^{h,f}, A. Gaddi^b, C. Gatto^c, P. Gauzzi^h, E. Gero^b, S. Giovanella^h, V. Golovyatuk^d, E. Gorini^d, F. Grancagnolo^d, W. Grandegger^b, E. Graziani^k, U. v. Hagel^c, R. Haydar^b, M. Imhof^c, M. Incagli^g, C. Joram^c, L. Keeble^b, W. Kim^l, W. Kluge^c, F. Lacava^h, G. Lanfranchi^h, P. Laurelli^b, J. Lee-Franzini^{b,l}, G. Margutti^h, A. Martini^b, A. Martinis^m,

M.M. Massai^g, R. Messiⁱ, L. Merola^c, A. Michetti^h, S. Miscetti^b, S. Moccia^b, F. Murtas^b, M. Napolitano^c, A. Nisati^h, E. Pace^b, G.F. Palamà^d, M. Panareo^d, L. Paoluziⁱ, A. Parri^b, E. Pasqualucciⁱ, M. Passaseo^h, A. Passeri^k, V. Patera^b, F. Pelucchi^b, E. Petrolo^h, M.C. Petrucci^h, M. Piccolo^b, M. Pollack^l, L. Pontecorvo^h, M. Primavera^d, F. Ruggieri^a, P. Santantonio^b, R.D. Schamberger^l, A. Sciubba^h, F. Scuri^m, A. Smilzo^c, S. Spagnolo^d, E. Spiriti^k, C. Stanescu^k, L. Tortora^k, P.M. Tuts^f, E. Valente^h, P. Valente^b, G. Venanzoni^g, S. Veneziano^h, S. Weseler^c, R. Wieser^c, S. Wölfle^b, A. Zallo^b.

^a Dipartimento di Fisica dell'Università e Sezione INFN, Bari, Italy.

^b Laboratori Nazionali di Frascati dell'INFN, Frascati, Italy.

^c Institut für Experimentelle Kernphysik, Universität Karlsruhe, Germany.

^d Dipartimento di Fisica dell'Università e Sezione INFN, Lecce, Italy.

^e Dipartimento di Scienze Fisiche dell'Università e Sezione INFN, Napoli, Italy.

^f Physics Department, Columbia University, New York, USA.

^g Dipartimento di Fisica dell'Università e Sezione INFN, Pisa, Italy.

^h Dipartimento di Fisica dell'Università e Sezione INFN, Roma I, Italy.

ⁱ Dipartimento di Fisica dell'Università e Sezione INFN, Roma II, Italy.

^j Dipartimento di Fisica dell'Università di Roma III e Sezione INFN, Roma I, Italy.

^k Istituto Superiore di Sanità and Sezione INFN, ISS, Roma, Italy.

^l Physics Department, State University of New York at Stony Brook, USA.

^m Dipartimento di Fisica dell'Università e Sezione INFN, Trieste/Udine, Italy.

References

- [1] A. General Purpose Detector for DAΦNE, The KLOE Collaboration, LNF-92/019 (1992).
- [2] The KLOE Detector, Technical Proposal, The KLOE Collaboration, LNF-93/002 (1993).
- [3] The KLOE Central Drift Chamber, Addendum to the Technical Proposal, The KLOE Collaboration, LNF-94/028 (1994).
- [4] G. Petrucci, KLOE Note 53 (March 1993).
- [5] G. Finocchiaro et al., Proc. 6th Int. Conf. on Advanced Detectors, Elba, Pisa, Italy, 1994.
- [6] A. Sharma and F. Sauli, CERN-PPE/93-51 (February 1993) and references therein.